# Nature of the "golden" phase of samarium sulfide

K. A. Kikoin

*I. V. Kurchatov Institute of Atomic Energy*

Examination of the problem of exciton states in the "black" (semiconducting) phase of SmS is used as a basis for a theory of the transformation of the ground state during the transition to the "golden" phase under pressure. According to this theory, golden-phase SmS is a narrow-gap semiconductor with valence band consisting of mixed valence states in which one of the $f$-electrons of each Sm ion has a definite probability of redistribution over $d$-orbitals that span a number of coordination spheres. The kinetic, optical, thermodynamic, and magnetic properties of golden-phase SmS are explained within the framework of this model.

PACS numbers: 71.25.Tn, 71.35. + z

## 1. INTRODUCTION

Recent experiments[1–3] on the kinetic properties of SmS under pressure have finally convinced us that the so-called "golden" phase of SmS, which exists in the pressure range $6 < P < 20$ kbar, is a distinct state that is intermediate between the normal superconducting phase with divalent $Sm^{2+}(f^6)$ ($P < 6$ kbar) and the metallic phase with altered valence ($P > 20$ kbar).

The currently established interpretation of the nature of this phase is that its ground state is a coherent superposition (since there is no experimental evidence for the inhomogeneity of the system) of the $f^6$ and $f^5d$ states, and that the spectrum of elementary excitations contains a gap or pseudogap that is responsible for the nonmetallic rise in resistance with decreasing temperature. The form of the $d$-function has been a matter for discussion. Two possibilities have been examined, namely, $d = d_c$ (band states, and $d = d_l$ (localized states) (see, for example, Refs. 4 and 5).

The difficulties of the model with band states (the so-called Anderson periodic model) arise because the statistics of the $f$ and $d_c$ states are different (atomic and Fermi, respectively), the coherent mixed-valency ground state cannot, in general, be constructed, and one must resort to approximations such as the coherent potential approximation,[4] in which the system is looked upon as a two-component "alloy" $f^6 + f^5d_c$. The gap (or pseudogap) in this model has a purely hybridizational character and its presence in the three-dimensional energy spectrum is difficult to verify.

It seems that the true mixed state must be sought along the path proposed by Kaplan and Mahanti[5] (KM) although their own variant of this theory, which gives ferroelectric order at $T = 0$ and has some difficulties with the Nernst theorem [see Eq. (3) in Ref. 6 and the discussion thereafter], cannot be accepted as realistic. In the present paper we put forward a localized mixing model which yields a coherent ground state and, at the same time, takes into account the actual properties of the SmS crystal and explains the origin of the exciton $d_l$ states. The model is used to provide a comprehensive explanation of the unusual kinetic, optical, and thermodynamic properties of the "golden" phase of samarium sulfide.

## 2. MODEL HAMILTONIAN FOR THE DIELECTRIC PHASE

The Hamiltonian for a system with mixed valency in the $f$-shell is usually written in the form

$$H = H_f + H_d + H_{fd}^{(1)} + H_{fd}^{(2)} + H_{eL}. \tag{2.1}$$

In the Hamiltonian $H_f$ for the inner shells of $f$-atoms in the cation sublattice of Sm, we must take into account two possible configurations, namely, $Sm^{2+}(f^6)$—the $^7F_0(\Gamma_1^+)$ singlet, and $Sm^{3+}(f^5)$—the $^6H_{5/2}(\Gamma_7^-)$ Kramers doublet. It is convenient to express $H_f$ in terms of projection operators:

$$H_f = \sum_m \left\{ |m0\rangle E_6 \langle m0| + \sum_M |mM\rangle E_5 \langle mM| \right\}, \tag{2.2}$$

where $E_{5,6}$ are the atomic level energies, 0 and $M$ label the atomic quantum numbers of the singlet and doublet ($M = \pm$), and $\mathbf{m}$ represents the coordinates of sites in the cation sublattice. In the band term, we shall take into account only the lower conduction band with a minimum at the $X$ point of the Brillouin zone which also exhibits only Kramers degeneracy (see, for example, Ref. 7):

$$H_d = \sum_{m,n,\sigma} t_{mn} d_{m\sigma}^+ d_{m\sigma} = \sum_{k\sigma} t_k d_{k\sigma}^+ d_{k\sigma}. \tag{2.3}$$

Since the $d$ and $f$ waves have opposite parities, the hybridization term $H_{fd}^{(1)}$ will mix only states centered on different sites:

$$H_{fd}^{(1)} = \sum_{mn}' \{ V_{mn} X_m^{0M} d_{n\sigma} + \text{h.c.} \} = \sum_k \{ V_k X_k^{0M} d_{k\sigma} + \text{h.c.} \}. \tag{2.4}$$

where $X_m^{0M} = |m0\rangle \langle mM|$ is the Hubbard projection operator, and

$$V_{mn} = \langle m0 | W | mM, n d\sigma \rangle$$

is the many-electron matrix element of the Coulomb interaction $W = e^2 |\mathbf{r} - \mathbf{r}'|^{-1}$, which is reduced to the one-electron form $\langle mf | V | nd \rangle$ by isolating the potential $V(r)$ of the $Sm(f^5)$ core. The form of the Coulomb interaction $H_{fd}^{(2)}$ and of the electron-lattice interaction $H_{eL}$ will be chosen below.

When given in the form (2.2)–(2.4), the Hamiltonian (2.1) is exceedingly inconvenient to deal with because the operators $d_{m\sigma}$ and $X_m^{M\sigma}$ have different statistics. We shall

0038-5646/83/090582-10$04.00    © 1984 American Institute of Physics    582

therefore exploit the device proposed in Refs. 8 and 9, i.e., to begin with, we shall take exactly into account the hybridization interaction in the one-electron band problem with core potential $V(f^5)$ in the Sm sublattice. As a result, we shall obtain two one-electron bands $\varepsilon_k^{(l,h)}$ with light and heavy carriers:

$$\varepsilon_k^{(l,h)} = \tfrac{1}{2}(\varepsilon_f + t_k) \pm [\tfrac{1}{4}(t_k - \varepsilon_f)^2 + V_k^2]^{\frac12}, \quad \varepsilon_f = E_6 - E_5. \quad (2.5)$$

The corresponding one-electron wave functions have the following form in the Bloch representation:

$$\psi_{hk} = u_k \psi_{fk} + v_k \psi_{dk}, \quad \psi_{lk} = u_k \psi_{dk} - v_k \psi_{fk},$$

$$u_k^2 = \frac{1}{2}\left\{ 1 + \mathrm{sgn}(\varepsilon_k - \varepsilon_f)\left[1 + \frac{4|V_k|^2}{(\varepsilon_k - \varepsilon_f)^2}\right]^{-\frac12}\right\}, \quad v_k^2 = 1 - u_k^2.$$

$$(2.6)$$

The initial and renormalized electron bands are shown schematically in Fig. 1 together with the symmetry of the states along the $\Gamma X$ line. The mixing of the $f$ and $d$ states occurs at all common points of the Brillouin zone, but does not occur at the points $(\Gamma, X)$ (Ref. 4).

The condition $D_h \ll \widetilde{U}$ is definitely satisfied for the narrow band $\varepsilon^{(h)}$ in the dielectric phase of SmS, where $D_h$ is the width of the band and $\widetilde{U}$ is the intraatomic Hubbard interaction between "heavy" electrons, so that allowance for $\widetilde{U}$ decreases by one-half the size of the phase-space cell, and the band $\varepsilon^{(h)}$ is actually a Hubbard subband containing $N$ electrons, where $N$ is the number of unit cells in the crystal. The upper band $\varepsilon^{(l)}$ is the usual Fermi conduction band. Thus, the band Hamiltonian for our semiconductor is

$$H_b = \sum_{m,n} \varepsilon_{mn}^{(l)} b_{m\sigma}{}^+ b_{m\sigma} + \sum_{mn} \varepsilon_{mn}^{(h)} Z_m{}^{0M} Z_n{}^{M0},$$

$$\varepsilon_{mm}^{(h)} = \varepsilon_f, \quad (2.7)$$

where, in contrast to $d_m$ and $X_m$, the symbols $b_m$ and $Z_m$ are used for the second-quantization operators of the hybridized states.

In the dielectric phase, so long as levels $\varepsilon_f$ and $t_k$ do not cross, hybridizational renormalization is small and can be taken into account by perturbation theory. The Wannier functions for the $h$ and $l$ bands can then be obtained from (2.6):

$$\psi_{hm} \approx \psi_{fm} + \sum_{n\neq m}{}' v_{mn}\psi_{dm}, \quad \psi_{lm} \approx \psi_{dm} - \sum_{n\neq m} v_{mn}\psi_{fn},$$

$$(2.8)$$

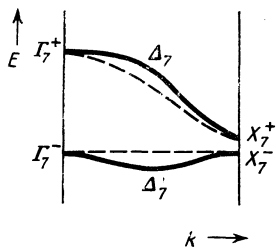$$v_{mn} = N^{-1}\sum_k V_k \exp i k(m-n)(t_k - \varepsilon_f)^{-1}.$$



FIG. 1. Structure of the forbidden band for SmS for $P = 0$.

As a result of hybridization, the $f$ and $d$ wave functions are distorted by the admixture of electron states of opposite parity, which are localized on neighboring states of the cation sublattice. The mixing integral increases exponentially with distance, and this enables us to write the $fd$ Coulomb interaction, responsible for the formation of excitons, in a simple form which leads to a solution for the exciton spectrum in an analytic form and, at the same time, takes into account all the physically significant processes:

$$H_{fd}^{(2)} = G\sum_{m\sigma} Z_m{}^{00} n_{lm\sigma} + \sum_{mn}\sum_{\sigma} \xi_{mn} Z_m{}^{00} n_{ln\sigma}$$

$$- \sum_{\sigma Mmn}{}'\sum_{\sigma} \xi_{mn} b_{m\sigma}{}^+ Z_m{}^{M0} Z_n{}^{0M'} b_{n\sigma'}$$

$$+ \sum_{\sigma Mmn}{}' \eta_{mn}(b_{m\sigma}{}^+ Z_m{}^{00} Z_n{}^{M0} + \text{h.c.}). \quad (2.9)$$

The first two terms in this expression describe the attraction between an electron and a hole on a given site and on neighboring sites of the cation sublattice, and the last two represent the transport of excitations and additional mixing, which were not taken into account in the formation of the electron-hole spectrum[1] (2.5). As for the intraatomic "Falicov" interaction, it is reasonable to suppose that $G < D_l$ (width of the "light" band), and the intersite interaction parameter can be obtained with the aid of (2.8) in the form

$$\xi_{mn} \approx U\left(\frac{V}{D_l}\right)^2 \Omega_0{}^{\frac12} \frac{e^{-2\kappa|m-n|}}{|m-n|}, \quad \kappa = \hbar^{-1}(2m_c^*\Delta)^{\frac12}, \quad (2.10)$$

where $\Omega_0$ is the volume of the unit cell, $\Delta$ is the gap width in the spectrum given by (2.5), $U \sim 6\text{–}8$ eV is the parameter in the initial intraatomic repulsion, $V \sim 0.1$ eV is the effective hybridization parameter, and $D_l \simeq 2$ eV. When we take into account the nearest-neighbor coordination number $z$ in the cation sublattice, we find that the pre-exponential factor reaches approximately 0.25 eV. In the derivation of the approximation (2.10) we took into account only that part of the interaction which was connected with the mixing of the $f$ states with the initial $d$ states in the conduction band.

## 3. EXCITONS IN THE DIELECTRIC PHASE

Possible formation of excitons in SmS and their influence on phase transitions with change in valency were discussed even in the earliest papers on unstable valence[10] but, strange as it seems, a microscopic analysis of the properties of excitons in such an unusual system as SmS is still lacking. In all papers (without exception) devoted to exciton states in SmS,[5,6,10–14] it is assumed without discussion that these are Frenkel states localized on a single site. In general, there is no justification for this assumption: even in alkali-halide crystals such as NaCl, whose ionicity is much greater, the Frenkel approximation is known to be invalid. On the other hand, the system parameters ($\varepsilon_0 = 5.9$, $m_c^* = 0.78$) are such that the effective-mass approximation cannot be expected to be valid either. It is thus natural to expect that the states in which we are interested are excitons of intermediate radius. This case is least amenable to theoretical analysis but, as will be shown below, the problem of the ground state of an exci-

ton with interaction whose range is restricted to the nearest coordination sphere can be solved practically exactly.

To find the exciton spectrum, it is convenient to transform in the Hamiltonian given by (2.7) and (2.9) to the hole representation of states in the heavy band. The role of the hole creation operator is then taken up by the operator of the change in the configuration $Z_m^{M0} \equiv f_{m\sigma}^+$. Thus, we shall solve the problem

$$(H - E_{ex})\Psi_{ex} = 0 \qquad (3.1)$$

with the Hamiltonian

$$H = \sum_{k\sigma} \varepsilon_k^{(l)} b_{k\sigma}^+ b_{k\sigma} - \sum_{k\sigma} \varepsilon_k^{(h)} f_{k\sigma}^+ f_{k\sigma}$$

$$-G \sum_{m\sigma\sigma'} f_{m\sigma}^+ f_{m\sigma} b_{m\sigma'}^+ b_{m\sigma'} - \sum_{mn}' \xi_{mn} f_{m\sigma}^+ f_{m\sigma} b_{n\sigma'} b_{n\sigma'}$$

$$- \sum_{mn\sigma}' \zeta_{mn} b_{m\sigma}^+ f_{m\sigma}^+ f_{n\sigma} b_{n\sigma}$$

$$+ \sum_{mn\sigma\sigma'}' \eta_{mn} f_{m\sigma} f_{m\sigma}^+ (b_{m\sigma'}^+ f_{n\sigma'}^+ + f_{n\sigma'} b_{m\sigma'}) \qquad (3.2)$$

(we are assuming the Coulomb renormalizations are included in the band spectrum). We shall measure the energy from the level $E_g = NE_6$. The wave function will be sought in the form

$$\Psi_{ex}(q) = S_q^+ |0\rangle, \qquad (3.3)$$

where $|0\rangle = \prod_m^N |m0\rangle$ is the ground-state wave function and $S_q^+$ is the exciton creation operator which can be written in the form

$$S_q^+ = N^{-1/2} \sum_m e^{-iqm} \sum_j F_q(j) f_{m\sigma}^+ b_{m+j,\sigma}^+$$

$$= N^{-1/2} \sum_k F_q(k) S_{q\sigma}^+ (k) |0\rangle, \qquad (3.4)$$

$$F_q(k) = \sum_j F_q(j) e^{-ikj}, \qquad S_{q\sigma}^+(k) = f_{k\sigma}^+ b_{k-q,\sigma}^+.$$

To be specific, all the spin directions were taken to be the same. Substituting (3.3) in (3.1), and multiplying from the left by $\langle 0|S_{q\sigma}^-(k)$, we obtain the Schrödinger equation for the envelopes

$$\sum_{k_1\sigma_1} F_q(k_1) \{\langle 0| (S_{q\sigma}^-(k), H] S_{q\sigma_1}^+(k_1) |0\rangle$$

$$+ \langle 0| H[S_{q\sigma}^-(k), S_{q\sigma_1}^+(k_1)] |0\rangle\} = E_{ex}(q) F_q(k) \delta_{\sigma\sigma_1}. \qquad (3.5)$$

As a rule, the use of operators of the form $X_m^{\lambda\lambda'}$ leads to additional difficulties because of the complexity of the commutation relations that they satisfy. In particular,

$$[f_{m\sigma}^+, f_{m\sigma'}]_+ = \{|m0\rangle\langle m0|\delta_{\sigma\sigma'} + |mM\rangle\langle mM'|\}\delta_{mm'}. \qquad (3.6)$$

However, this anticommutator becomes a delta function within $\langle 0|\cdots|0\rangle$, so that the operators $f_{k\sigma}$ can be treated like ordinary Fermi operators. Next, the second commutator in (3.5) gives simply the ground-state energy. Omitting, for the moment, the last two terms in (3.2), which describe the trans-

lation of electron-hole pairs and supermixing, and recalling the identity

$$\langle 0|S_{q\sigma}^-(k) S_{q\sigma'}^+(k')|0\rangle = \delta_{kk'}\delta_{\sigma\sigma'},$$

we obtain the following closed set of equations for the envelopes $F_q(k)$:

$$[\varepsilon_{k+q}^{(l)} - \varepsilon_k^{(h)}]F_q(k) - \sum_{k'} J(k-k')F_q(k') = (E - E_g)F_q(k),$$

$$\qquad (3.7)$$

$$J(k-k') = G + N^- \sum_{mn} \xi_{mn} e^{i(k-k')(m-n)}.$$

It is immediately clear from this that, even when only the attraction $G$ within the centers is taken into account, the exciton will not, in general, be of the Frenkel type. The set of equations given by (3.7) is then readily solved, and the following expressions are obtained for the exciton energy and wave function (see Ref. 15):

$$GN^{-1} \sum_k [E_{ex}(q) - E_k^{lh}(q)]^{-1} = -1, \qquad E_k^{lh}(q) = \varepsilon_{k+q}^{(l)} - \varepsilon_k^{(h)},$$

$$\qquad (3.8a)$$

$$F_q(j) = -GF_q(0)N^{-1} \sum_k [E_{ex}(q) - E_k^{lh}(q)]^{-1} e^{ikj}. \qquad (3.8b)$$

The quantity $F_q(0) = N^{-1}\sum_k F_q(k)$ can be looked upon as a normalizing factor. In contrast to the one-dimensional Egri problem,[15] a discrete exciton level appears, in our case, only for $G > G_c$. The threshold value $G_c$ can be estimated by solving the equation

$$\int \frac{dE S_0(E)}{\chi(E)} = G_c^{-1}, \qquad \chi(E) = [(E + \Delta + G)^2 + 4V^2]^{1/2}, \qquad (3.9)$$

where $S_0(E)$ is the density of states in the renormalized conduction band $\varepsilon_{dk}$. Replacing $S_0(E)$ with the effective constant $2D_l^{-1}$, we obtain the following equation for $G_c$:

$$\frac{2G_c}{D_l} \ln \frac{2(D_l + \tilde\Delta)}{\tilde\Delta + (\tilde\Delta^2 + 4V^2)^{1/2}} = 1, \qquad \tilde\Delta = \Delta + G. \qquad (3.10)$$

Thus, the system has a discrete exciton level when

$$e^{D_l/2G} < D_l/\max\{\tilde\Delta, V\}. \qquad (3.11)$$

If we assume that $\{\bar\Delta, V\}$ is approximately equal to 0.2 eV, we obtain $G_c \approx 0.43$ eV.

When $G > G_c$, the envelope $F_0(R)$ has the following approximate dependence on distance:

$$F_0(R) \sim F_0(0) R^{-1} e^{-\varkappa R}, \qquad \varkappa = \hbar^{-1}\{2m_c^*[\bar\Delta - E_{ex}(0)]\}^{1/2}.$$

$$\qquad (3.12a)$$

Hence, it is clear that the Frenkel exciton appears only when the binding energy is approximately 3 eV, which is clearly an unrealistic figure. The difference from the Frenkel exciton becomes greater still when the attraction $\xi(R)$ between the sites is taken into account. When the interaction $\xi(R)$ is taken into account only for nearest neighbors, so that $\xi(a/\sqrt{2}) \equiv \xi$, and neglecting the contribution to the envelope of all sites outside the second coordination sphere, we can transform in (3.7) to the site representation and thus obtain a set of thirteen equations in the $F(j)$:

$$F(0) = -\xi (1+GD_{00})^{-1} \sum_m D_{0m} F(m),\qquad (3.13a)$$

$$F(j) + \xi \sum_m \left( D_{jm} - \frac{GD_{j0}D_{0m}}{1+GD_{00}} \right) F(m) = 0, \quad m, j \neq 0 \quad (3.13b)$$

(we have confined out attention to the case $q = 0$, which is important for our purposes). In these expressions,

$$D_{jm}(E) = N^{-1} \sum_k [E - E_k^{lh}(0)]^{-1} \exp ik(j-m), \quad (3.14)$$

where the sum is evaluated over sites in the second coordination sphere.

The energy levels of the intermediate-radius exciton are classified in accordance with the irreducible representations of the point group of the crystal, so that (3.13b) can be transformed to a block-diagonal form by going over to the irreducible basis of the group $O_h$. However, the fully-symmetric solution

$$F_s = F(0) + \sum_j F(j) = F(0) + F_{1s}, \qquad (3.15)$$

in which we are interested here and which corresponds to the lowest state of the exciton, can be found directly without resorting to the methods of group representation theory. Actually, we shall use the fact that the lattice Green functions (3.14) that appear in (3.13) and their combinations depend only on $|j| = a/\sqrt{2}$:

$$D_{01} \equiv D_{0j} = N^{-1} \sum_k (E - E_k^{lh})^{-1} e^{-ikj},$$

$$D_1 \equiv \sum_j D_{0j} = N^{-1} \sum_k (E - E_k^{lh})^{-1} s(k), \qquad (3.16)$$

$$D_2 \equiv \sum_m D_{jm} = N^{-1} \sum_k (E - E_k^{lh})^{-1} e^{-ikj} s(k),$$

where $s(k)$ is the formfactor which, in the case of the fcc sublattice, is given by

$$s(k) = \sum_j e^{ikj} = 4 \left( \cos \frac{k_x a}{2} \cos \frac{k_y a}{2} + \cos \frac{k_y a}{2} \cos \frac{k_z a}{2} \right. $$
$$\left. + \cos \frac{k_z a}{2} \cos \frac{k_x a}{2} \right).$$

Having constructed the solution $F_s$ of (3.13b), we obtain the equation for the energy of the singlet exciton:

$$1 + GD_{00}(E_{ex})$$
$$= -\xi \{ D_2(E_{ex}) - G[D_1(E_{ex})D_{01}(E_{ex}) - D_2(E_{ex})D_{00}(E_{ex})] \},$$
$$(3.17)$$

in whose right-hand side are gathered the terms responsible for the renormalization of the level $E_{ex}(0)$ by the interaction between the sites. Equation (3.13a) presents us with an expression for the envelope, which replaces (3.8b):

$$F_{1s} = -\frac{GD_1}{1+\xi D_2} F(0) \qquad (3.18)$$

with the normalization

$$F^2(0) + zF_{1s}^2 = 1. \qquad (3.19)$$

It is clear from the last two equations that allowance for the

Coulomb interaction between sites leads to the splitting of the exciton spectrum in accordance with the representations of the point group of the crystal. It also leads to an overall raising of the exciton states $(D_2(E_{ex}) < 0)$ and to a corresponding redistribution of charge density, i.e., to additional transport of negative charge in the electron-hole pair from the central cell to neighboring atoms in the cation sublattice.

Exciton dispersion $E_{ex}(q)$ is limited by the exchange term in the Hamiltonian (3.2) and by the dispersion of the lower band[15] $\varepsilon_k^{(h)}$. It is very small and will be unimportant for our ensuing analysis.

The complete exciton wave function (3.3) is constructed with the aid of the vector-addition scheme for point groups from the wave functions of the $f^5$ ion and the electron orbitals $\beta_{m\lambda}$. When $q = 0$, the wave function is given by

$$\Psi_{ex}^\Gamma(0) = N^{-1} \sum_m |mf^5\Gamma', B_{m\lambda}; \Gamma\rangle,$$

$$(3.20)$$

$$|B_{m\lambda}\rangle = F(0) b_{m\sigma}^+ |0\rangle + F_{1s} \sum_j a_j^\lambda b_{m+j,\sigma}^+ |0\rangle,$$

where $a_j^\lambda$ are the coefficients in the transformations of of the Wannier functions $\psi_{l,m+j}$ to the irreducible representation $\lambda$ of the point group, $\Gamma'$ is the corresponding representation for the $f^5$ ion, and $\Gamma = \Gamma' \otimes \lambda$. Hence, it is clear that the exciton can be taken to the higher-lying state in two ways: either by exciting the $f$-shell $(\Gamma')$ or by modifying the envelope $(\lambda)$.

The following picture of the behavior of the exciton wave function in the semiconducting phase of SmS as a function of pressure $P$ is thus seen to emerge from the foregoing. As $P$ increases, the gap $\Delta$ in the electron spectrum (2.5) is reduced, and this leads to an increase in the degree of mixing of the $d$ and $f$ states in the wave functions (2.6), i.e., to an increase in the contribution of the $f$ component to the wave functions of the conduction electrons and, hence, to an increase in the parameter (2.10) of the Coulomb interaction between the sites. When a discrete exciton level $(G > G_c)$ is present in the initial state with $P = 0$, the level will fragment with increasing $P$, and the radius of the exciton will increase as a result of negative-charge transport to neighboring Sm atoms, whereas the positive charge will, as before, be essentially localized in the single cell. In the final analysis, the reduction in the size of the band gap of the semiconductor will ensure that the exciton binding energy will exceed the size of this gap, i.e., we shall have exciton instability of the crystal.

## 4. GOLDEN PHASE: NARROW-GAP SEMICONDUCTOR WITH MIXED VALENCE

We have found in the last section that the presence of discrete exciton levels in the spectrum unavoidably leads to the onset of exciton instability of the "black" semiconducting phase of SmS, well before the gap is reduced under pressure. The traditional way of treating exciton instability is based on the application of perturbation theory and BCS-type approximations, but this is invalid in our case for a number of reasons. First, in a system described by the Hamiltonian (3.2), which does not conserve the number of elec-

585   Sov. Phys. JETP **58** (3), September 1983

K. A. Kikoin   585

tron-hole pairs because of the presence of its last term, the phase transition, in accord with the general ideas of exciton instability, will be of first order[16] (see also Ref. 17). Actually, isomorphous transformation in a direct-gap semiconductor reduces to a redistribution of electron density in the $d$ and $f$ shells of the Sm ions, accompanied by a reduction in the volume of the unit cell without the appearance of any new order parameter. Second, as will be seen from the ensuing analysis, the mixed valence state can be obtained only by abandoning the self-consistent field approximation. Finally, it is known that perturbation theory encounters major mathematical difficulties when $m^* \to \infty$ in one of the bands. It seems to us, therefore, that the simplest way of finding a realistic wave function for the ground state constructed above is to use the variational method.

Thus, we shall seek this function in the form

$$|\Psi\rangle = \prod_m^N (\cos\theta + \sin\theta S_m^+)|0\rangle \equiv \prod_m A_m^+|0\rangle,$$

$$S_m^+ = \frac{1}{\sqrt{2}}\sum_\sigma f_{m\sigma}^+ B_{m\sigma}^+, \quad B_{m\sigma}^+ = F(0)b_{m\sigma}^+ + F_{1s}\sum_j b_{m+j,\sigma}^+. \quad (4.1)$$

This trial function relies on the assumption that, first, the phase transition does not involve any essential rearrangement of the "orbitals" $B_m$ and, second, the black–phase excitons are still sufficiently localized at the critical pressure $P = P_c$, and we can confine ourselves to inclusion of the nearest neighbors alone. The second restriction is dictated only by considerations of mathematical simplicity, and does not have a decisive effect on the physical picture. The choice of the directions of $\sigma$ is dictated by the requirement that the states to be mixed transform under the same representation as the original representation (see below).

Trial functions with localized orbitals have already been examined in the literature[18-20] in relation to special cases of the Hamiltonian (3.2). It was noted[18b] that the "localized" basis gives a lower variational energy than the standard basis with Bloch functions. However, it has a basic disadvantage, namely, the trial functions are not orthogonal. In fact, in our case, we have from (4.1) and (3.19)

$$[B_m^+, B_m]_+ = 1, \quad [B_m^+, B_{m+j}]_+ = 2F(0)F_{1s} + yF_{1s}^2 \equiv \alpha, \quad (4.2)$$

where $y$ is the number of nearest neighbors common to the sites $\mathbf{m}$ and $\mathbf{m}+\mathbf{j}$ ($y = 4$ for the fcc lattice). It has been shown[19,20] that, in the metallic case (when, in the ground state, there are electrons in the conduction band), one has to take into account excluded-volume type effects, which sharply complicates the situation and takes us back to the problem of the "Kondo-Anderson lattice." It seems to us that the situation is much simpler in the dielectric ground state. The excluded-bond effect does not then arise because the formation of the orbital $B_m$ involves only the $1/z$ part of the Wannier amplitude $b_{m+j}$. The main problem that we now encounter is the "nonorthogonal catastrophe," well known in the Heitler-London-Heisenberg model.[21]

Actually, if we evaluate the ground-state energy

$$\bar{E}_g = \langle \Psi|H|\Psi\rangle / \langle \Psi|\Psi\rangle \quad (4.3)$$

with the trial function (4.1), both the numerator and the de-

nominator contain diverging series $\sim (N\alpha^2)^k$. In principle, the problem can be solved because terms $\sim N^k, k > 1$ in both the numerator and the denominator in (4.3) almost completely cancel out, and the remaining corrections which are $\sim N$ can often be found explicitly. In the case of weak overlap this procedure can be implemented in our problem as well. Details of how diverging terms can be removed from the variational expression for the ground-state energy will be published elsewhere, and only an outline of the computational scheme will be given here.

The expression given by (4.3) with the Hamiltonian (3.2) and trial functions (4.1) can be written in the form

$$\bar{E}_g - E_g = \langle\Psi|\Psi\rangle^{-1}\Big\{\sum_1 \langle\Psi|\Big(\prod_{m\neq 1} A_m^+\Big)[H, A_1^+]|0\rangle$$

$$+ \frac{1}{2}\sum_{11'}\langle\Psi|\Big(\prod_{m\neq 1,1'} A_m^+\Big)[[H, A_1^+], A_{1'}^+]|0\rangle\Big\}. \quad (4.4)$$

If we exploit the fact that the operator $[H, A_1^+]$ can generate only one-exciton excited states, whereas $[[H, A_1^+], A_1^+]$ generates two-exciton states, we can factorize (4.4) as follows:

$$N^{-1}(\bar{E}_g - E_g) \approx \Phi_1 \Delta_{ex} \sin^2\theta - \Phi_2 J \sin^4\theta - \Phi_3 M \cos\theta \sin\theta,$$

$$\Delta_{ex} = E_{ex}(0) - E_g. \quad (4.5)$$

The first term in this expression describes the "crossing" of the levels $E_{ex}$ and $\varepsilon_f$, whereas the second the third terms represent interaction between the excitons and supermixing effects with the corresponding energy parameters

$$J \approx 4GF_1^2 F_0^2 z, \quad M = 2F_1\eta z, \quad [\eta \equiv \eta(a/\sqrt{2})], \quad (4.6)$$

where $\Phi$ are the nonorthogonality parameters

$$\Phi_1 = \frac{\langle 0|S_1^-(\Pi A_m^-)(\Pi' A_m^+)S_1^+|0\rangle}{\langle\Psi|\Psi\rangle},$$

$$\Phi_2 = \frac{\langle 0|S_1^- S_{1'}^-(\Pi'' A_m^-)(\Pi'' A_m^+)S_{1'}^+ S_1^+|0\rangle}{\langle\Psi|\Psi\rangle} \quad (4.7)$$

$$\Phi_3 = \frac{\langle 0|(\Pi' A_m^-)(\Pi' A_m^+)|0\rangle}{\langle\Psi|\Psi\rangle}.$$

The primes on $\Pi$ indicate the absence from the product of one or two operators $A_m$ (the quantities $\Phi$ do not, of course, depend on the choice of the site).

The factors given by (4.7) can be evaluated by the well-known Löwdin-Carr procedure of expansion in terms of the minors of the determinants in their numerators (see Ref. 21). For weak overlap,

$$\alpha z^{1/2} \sin^2\theta \ll 1 \quad (4.8)$$

this procedure gives the following result in the lowest order in $\alpha$:

$$\bar{E}_g - E_g = N\{n_d \Delta_{ex}(1 - z\alpha^2 n_d) - n_d^2 J - [n_d(1 - n_d)]^{1/2}M + 0(n_d^{1/2})\}. \quad (4.9)$$

This expression includes the parameter $n_d = \sin^2\theta$, which can be interpreted as the density of electrons on the localized orbitals. Higher-order terms in the density are not written out because they do not affect the qualitative picture of the phase transition. We see thus that nonorthogonality intro-

duces in the ground-state energy a correction that is quadratic in the density and can, at least in principle, contribute the establishment of mixed valence in the system (see below).

In the case of stronger mixing, when (4.8) is violated, the procedure for evaluating the corrections is much more complicated, but we shall assume that the transition can be understood qualitatively by considering the example of the simple situation examined above. The expression (4.9) reproduces the phenomenological functionals $E\{n_d\}$ introduced in Refs. 14 and 22, where $n_d$ was replaced by the concentration of the free electrons or bound excitons. However, it is important to emphasize that the microscopic justification of (4.9) in our theory is quite different from that in the Kuroda-Bennemann approach.[14] We have already had occasion to note[8] that the analogy with dilute alloys, in which a mixed-valence state is treated as a mixture of the ions $Sm^{2+}$ and $Sm^{3+}$ (see, for example, Ref. 4), will not contribute anything useful to the construction of the coherent ground state. This is also valid for the exciton mechanism of the transition. The concept of localized quasimolecular excitons, whose concentration increases as one approaches the phase transition point,[11,14] seems to us to be as unproductive in the description of the ground state as the alloy analogy in the case of the Anderson lattice. In reality, an exciton is excited in a homogeneous system not on an individual site, but simultaneously all over the crystal, and this dictates the choice of the trial function in the form given by (4.1).

A phase transition in the system with ground state described by the density functional (4.9) can be either of first order or continuous. However, in the real case of SmS, we cannot confine ourselves to consideration of electron subsystem alone, and we must take into account the electron-lattice interaction because the radius of the Sm ions varies appreciably in the transition when the valence is changed. The lattice mechanism for the transition is based on the old, Zachariasen-Pauling idea, put forward in connection with the $\alpha$-$\gamma$ transformation in Ce: the isomorphous transition is looked upon as the "crushing" of the shells of REM ions, as a result of which ions of smaller radius are packed in the new phase into the same lattice. Extending this idea to the "exciton" transition in SmS, Kaplan and Mahanti[5] have written down the following phenomenological expression for the volume-dependent energy:

$$E(V) = \frac{1}{2}[B_2(V-V_2)^2 \cos^2\theta + B_3(V-V_3)^2 \sin^2\theta] + \text{const},$$

$$(4.10)$$

where $V_2$, $V_3$ are the specific volumes per $Sm^{2+}$ and $Sm^{3+}$ ion, respectively, $B_2$ and $B_3$ are the corresponding compressibilities, and the parameter $\theta$ is a measure of the fraction of these and other ions in the crystal.

In our model, the electron-lattice interaction manifests itself in at least three ways: the deformation of the lattice changes the energy gap $\Delta_{ex}$, the depth of the exciton level $E_{ex}$, and the magnitude of the Green functions $D_{mj}$ that depend exponentially on the lattice constants. Thus, an increase in pressure is accompanied by an increase in the fraction of negative charge on the periphery of the exciton quasimolecule, and this means that the mixing constant $M$ in (4.6) increases, too. Next, assuming that the energy gap $\Delta$
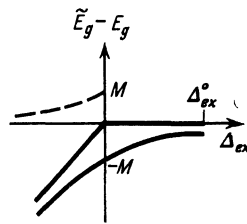


FIG. 2. Ground-state energy as a function of the specific volume (see text). Dashed line—exciton energy in the modified state.

decreases with increasing pressure much more rapidly than the fragmentation of the exciton level $E_{ex}$, we can use the expression

$$\Delta_{ex}(V) = \Delta_{ex}^0 + D\delta,$$

$$(4.11)$$

where $\delta = (V - V_2)/V_2$ is the relative change in the volume and $D$ is of the order of the deformation potential.

The phase transition problem for a system described by (4.9)–(4.11) has been investigated in great detail[6,13,14] and we shall therefore confine ourselves to a brief examination of the effect of the leading interactions on the nature of this transition. To estimate the range of possible values of the parameters of the problem, we begin with the very crude approximation in which $J$, $M = 0$ and the change in the elastic constants during the transition is ignored. In this variant with simple level crossing, the ground-state energy is given by

$$E(P, \delta) = E_g + \frac{1}{2}B_2V_2\delta^2, \quad |\delta| < |\delta_1|,$$

$$(4.12)$$

$$E(P, \delta) = E_g + \frac{1}{2}B_2V_2\delta_2 + D(\delta-\delta_1), \quad |\delta| > |\delta_1|$$

(broken line in Fig. 2), where $\overline{\delta}$ is the equilibrium value of $\delta$ for given $P$, determined by the condition $P = -dE/dV$, and $\delta_1$ is the value of $\delta$ for which the gap (4.11) closes. The equation of state is

$$\delta = -P/B_2, \quad |\delta| < |\delta_1|,$$

$$\delta = -(P+DV_2^{-1})/B_2, \quad |\delta| > |\delta_1|.$$

$$(4.13)$$

Of course, this equation will reproduce the actual equation of state only in a very schematic way (fine lines in Fig. 3a), but it does yield quite reasonable values for its parameters. For example, if we take $D = 4.5$ eV, $V_2 = 60$ Å³, and $B_2 = 500$ kbar, we find that the jump in the volume that accompanies the phase transition, and is shown by (4.13) to be $\Delta\delta = D/B^2V^2$, turns out to be 0.24 (the experimental value is $\Delta\delta = 0.13$). In the simplified linear model, the critical pressure for the transition is given by $P_c = -B_2/\delta_1$. Using the experimental result $P_c = 6.5$ kbar, we obtain the upper limit for the energy of the exciton state: $E_{ex} \lesssim \Delta_0 - |\delta_1|D = 0.17$ eV (for $\Delta_0 = 0.23$ eV). In reality, the exciton level will lie higher because the modulus $B_2$ will be softened as $P_c$ is approached, but the limiting value of $E_{ex}$ seems reasonable, and the nearest-neighbor approximation realistic.

We now introduce hybridization. Minimization of the functional (4.9) without allowing for the correlation effects $\sim n_d^2$ yields the following expression for the energy:
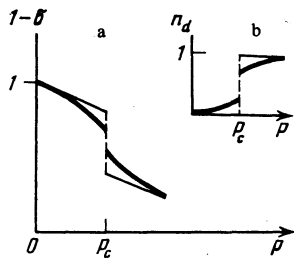
FIG. 3. $P-V$ and $P-n_d$ diagrams for SmS.



FIG. 4. Structure of mixed-valence state.

$\bar{E}_g=E_g+{}^1\!/_2(\Delta_{ex}-(\Delta_{ex}{}^2+M^2)^{1/2})$, $n_d={}^1\!/_2[1-\Delta_{ex}(\Delta_{ex}{}^2+M^2)^{-1/2}]$.

(4.14)

If we neglect the contribution to the compressibility due to the orbitals $B_m$, the elastic energy will be largely determined by the core, which includes the $f$-shells and should be of the form given by (4.10). According to Refs. 6 and 13, a phase transition in a system described by (4.10) and (4.14) can be either discontinuous or continuous. It is clear from Fig. 2 that the role of hybridization is to smooth out the transition (the broken line is replaced with a hyperbola). The jump in the volume is then reduced (thick lines in Fig. 3a) and the "valence" $n_d$ on either side of the transition point is no longer an integer (thick lines in Fig. 3b). Hybridization plays a comparable role in the dielectric-metal transition.[23]

The "interexciton" attraction appears in our model only when we leave the self-consistent field approximation (compare this with Ref. 17). It gives rise to a tendency toward a discontinuous transition but, because of hybridization, a transition with a change in valence, but without allowance for elastic energy (4.10), remains continuous. In our theory, the orthogonalization correction in (4.9) plays a role similar to the anharmonic contribution to elastic energy.[22] We have $\Delta_{ex}<0$ for $|\delta|>|\delta_1|$, so that the effect of orthogonalization reduces to the smoothing out of the transition and the establishment of intermediate valence. Thus, the hybridization and orthogonalization corrections facilitate, in our theory, the replacement of the discontinuous by a continuous transition along the series SmS-SmSe-SmTe.

The state with mixed valence appears mainly as a result of Coulomb supermixing. The nature of the mixing process is clearly demonstrated by the form (4.6) of the matrix element of this interaction: as in the Hartree-Fock hybridization (2.8), this matrix element involves only states connected with neighboring sites and, mainly, due to the $f$-components of wave functions in the conduction band. Thus, in our model, the realization of a mixed-value state signifies that one of the electrons on the divalent ion $Sm^{2+}$ ($f^6$) can be partly redistributed over the nearest sites of the Sm sublattice, but still remains bound to its own site (Fig. 4). According to (4.1), the wave function $\psi_m\{f^6\}$ then acquires an admixture of $\psi_m\{f^6B\}$ in which the orbital $B$ has the following form when expressed in terms of the original $d$- and $f$-wave functions [see (2.8)]:

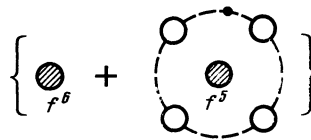$\psi_{Bm}\approx F(0)\psi_{dm}+F_{1s}\sum_s(\psi_{d,m+l}-v_{m+l,m}\psi_{fm})$ (4.15)

(the contribution due to $f$-functions from neighboring sites is neglected). It is readily seen that the added state has the same set of quantum numbers as the $f^6$ configuration. In fact, functions from sites in the second coordination sphere comprise fully symmetric combinations, so that the $f$ component of the orbital (4.15) transforms in accordance with the representation of the rotation group with $l=3$ and, together with the spin function, forms a state with total angular momentum $j=5/2$, which is dictated by the scheme used to combine the angular momenta of the states $f^5({}^6H_{5/2})$ and $f^1(j=5/2)$ into the singled ${}^7F_0$. As noted by Stevens,[18a] the $j=5/2$ combination can be made up of $d$ functions from the second coordination sphere [second term in (4.15)]. As a result, we have the following expression for the wave function of the Sm ion at the site $m$ in a mixed-valence state:

$\Psi_m=\cos\theta|f^6$; ${}^7F_0\rangle+\sin\theta|f^5({}^6H_{5/2})$, $B({}^1d_{5/2})$; ${}^7F_0\rangle$. (4.16)

Coherent Bloch waves made up of these combinations are, in fact, the wave functions of valence electrons in the golden phase of samarium sulfide. In addition to the "bonding" state (4.16), it is also possible to constuct an "antibonding" state of the $f^6-f^5B$, which is an exciton in the new phase. As in the usual theory of excitonic dielectrics,[16] collective excitations are separated from the ground state by a gap (dashed line in Fig. 2).

The variational procedure that we have used does not enable us to estimate the rearrangement of the band continuum $b_k$ but, when this is neglected, the gap separating it from the valence states can be estimated from the expression

$\Delta<\Delta_{ex}{}^c+M$, (4.17)

where $\Delta_{ex}^c$ is the critical value of $\Delta_{ex}$ corresponding to the exciton instabi9lity. Thus, in our model, the golden phase of SmS is a narrow-gap semiconductor with a specifically constructed valence band, whose symmetry is identical with that of the normal black phase.

## 5. GOLDEN PHASE. INTERPRETATION OF EXPERIMENTAL DATA

We must not overestimate the fact that the mixed-valence "excitonic" dielectric model explains the $PV$ diagram of the phase transition: it shares this distinction with practically any theory of a transition with a change in valence that involves the crossing of two levels or the entry of a level into the band. The criterion for choosing between competing models is their ability to explain numerous unusual experimental facts in an unified rather than fragmented manner. Examination of all the variants of the theories proposed so far forces us to acknowledge that the KM model[5,6] is the only one that has not been unsuccessful in attempting to provide a unified explanation of the properties of the golden phase of SmS. To be sure, this model is not free of the fundamental
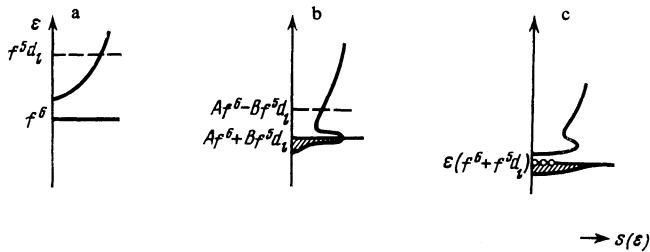
FIG. 5. Density of electron states in black (a) and golden (b) SmS in the KM model, and in golden SmS in our model (c).

deficiencies mentioned in the Introduction. We shall show in this section that our mixed valence model of a semiconductor is free of these shortcomings, and will put forward our own interpretation of the kinetic, optical, and magnetic properties of the intermediate phase of samarium sulfide.

We note, to begin with, that our model does not predict ferroelectric order at $T = 0$, the possibility of which in the KM model is its most objectionable feature. The physical reason for this ordering in the KM theory is the interaction between the dipole moments that appear in each cell as a result of mixing of states of different parity. In our case, we showed in the last section that the fully-symmetric orbitals form a singlet ground state with zero angular momentum.

Second, to explain the finite conductivity of the golden phase and its metallic reflectance, Kaplan and Mahanti[5] propose that roughly 0.1 of an electron per site remains in the conduction band after the transition. At the same time, they have had to assume that a localized mixed-valence level crosses the band near its bottom (Fig. 5). Hence, it follows that the ground-state wave function is[5]

$$\widetilde{\Psi} = (Af^6 + Bf^5 d_l)^{N(1-b)} (f^5)^{Nb} (d_k)^{Nb}, \tag{5.1}$$

where $b \sim 0.1$ is the fraction of delocalized electrons (in the zero-order approximation). This expression corresponds to nonzero configurational entropy, and Kaplan and Mahanti do not propose a satisfactory method of avoiding the violation of Nernst's theorem.

The level scheme shown in Fig. 5b has been criticized for another reason as well: it was considered that it is in conflict with the experimentally observed rise in the concentration $n_c$ of conduction electrons from $10^{20}$ to $10^{22}$ cm$^{-3}$ that accompanies the transition to the golden phase.[24] However, the data reported in Ref. 24 were obtained at room temperature, and it is now clear that they are unrelated to the properties of the system in the ground state: Hall-effect measurements[3] have shown that, at $T \simeq 15$ K, the sign of the carriers changes, and the hole concentration amounts to $6 \times 10^{19} - 9 \times 10^{19}$ cm$^{-3}$ as $T \to 0$, which is roughly the same as the impurity concentration in the system. However, these data also contradict the level scheme shown in Fig. 5b.

It seems to us that the most intriguing peculiarities of the golden phase of SmS (its kinetic properties) can only be understood by taking into account the presence of impurities (and stoichiometric defects) in the real crystals of samarium sulfide. We recall that the temperature dependence of the resistance $R (T)$ of golden SmS is nearly exponential for $T > 5$ K, and passes through a maximum as the temperature is

reduced still further. It reaches 800–2300 $\mu\Omega \cdot$ cm at $T \simeq 1$ K (depending on the magnitude of $P$). In our view, this temperature dependence of the resistance is the combined result of two charge-transfer mechanisms, namely, hole conduction for $T < 5$ K and electron conduction in the $d$ zone, which rapidly increases with increasing $T$ in a thermally-activated manner and shunts the low-temperature hole conduction. The latter can be ascribed to donor levels found in the black phase of SmS.[25] However, data on electron specific heats (see below) force us to assume that there are holes in the "exciton" band $\varepsilon_{ex}$ $(f^6 f^5 d)$ (Fig. 5c). The presence of holes is most likely associated with the acceptor action of intrinsic defects whose concentration is about 1% (we recall that, as a rule, even the black phase exhibits hole conductivity at low temperatures[25,26]). We shall not examine here the specific question of conduction in the narrow hole band with strong correlation and its dependence on $P$ and $T$. The exponential reduction in $R$ for $T > 5$ K, which is connected with the activation of carriers across the gap, can be partially masked by the temperature dependence of the mobility.[3] We also note that our model predicts that, as $T \to 0$, the resistance should increase with increasing degree of purity of the crystal.

The next group of properties relates to the optical and x-ray spectra. They include experimental data on optical absorption that provided Kaplan and Mahanti with the basis for the level scheme shown in Figs. 5a and b. In this connection, we must note that the $d_l$ exciton states (Fig. 5a) have been recorded[27] as the final states in the optical transition $f^6 \to f^5 d$, so that they must have different parities as compared with $f^6$. At the same time, hybridization with a center of inversion occurs in a cubic crystal only between states of the same parity, so that the experiment reported in Ref. 27 can serve as a justification for the localized mixing model only if it is assumed that forbidden transitions have been observed. On the other hand, our view is that these transitions correspond to the excitation of high-lying exciton states (3.1) with $J \neq 0$. In the golden phase, the frequencies of these transitions are shifted as compared with the black phase, and this may well be the explanation of the disappearance of the corresponding lines from the experimental spectra[28] for $P > P_c$. In the light of (4.16), which gives the ground-state wave function, we can readily understand the absence from the golden phase of intracenter transitions that correspond to the $f^5$ configuration.[28]

The metallic nature of the reflection coefficient (the presence of a plasmon edge at $\omega \simeq 2.5$ eV) is very puzzling in the light of data obtained as a result of studies of transport effects, but has an unexpectedly simple solution in our model. Although there are no free electrons in the golden phase, the electron density distribution on the quasimolecular orbits (4.1) (Fig. 4), on which all the electrons that have left the $f^6$ shells reside, is not very different from the metallic distribution. In fact, these orbitals may be even less localized than in our simple model, so that the natural frequencies of electrons in the orbitals may lie in the infrared region. As a result, the frequency of their collective vibrations can be determined from the expression $\omega_p^2 = 4\pi n_d ne^2/m$, where $n = 2 \times 10^{22}$ cm$^{-3}$ is the concentration of samarium atoms

in the crystal. When $n_d \simeq 0.7$, we have $\hbar\omega_p \approx 3.8$ eV, which is in reasonable agreement with experiment if we take into account possible renormalization of the plasmon frequency by interband transitions.

The anomalously high temperature coefficient of electron specific heat, $\gamma = 145$ mJ/mole $\cdot$ deg, in our model can be naturally related to the contribution of hole excitations in the "exciton" band, which also determine the kinetic properties of the system for $T < 5$ K (see above). We note, by the way, that the linear temperature dependence $C(T)$ is observed precisely in this interval of temperature, and thereafter the specific heat rises relatively sharply,[29] which probably indicates that a new group of electron levels comes into play. The quantity $\gamma$ cannot, as yet, be accurately calculated because the question of Fermi excitation in a band whose ground state is described by wave functions of the form of (4.16) requires special analysis. It is clear, however, that this band is very narrow and that the effective hole mass is strongly renormalized by different interactions. In particular, the strong Hubbard-type Coulomb interaction can be taken into account in the gas approximation.[8,9] Estimates[3] of the effective mass, based on experimental values of $\gamma$ and $n_p \sim 10^{20}$, yield $m^* \simeq 300$–$500$. Kaplan and Mahanti[5] have put forward in their review some ideas that explain how electron and polaron interactions can reduce the width $\sim 5$ eV of the original band to $\sim 500$ K and increase the effective mass of the carriers to about 90. Allowance for the Fermi-liquid renormalization and for the degeneracy factor $g = 3$ connected with the presence of several valleys yields a figure for $m^*$ that is of the required order, but proper quantitative estimates must be underpinned by a regular theory.

The presence of the linear contribution to the electron specific heat and entropy due to carriers in the narrow band enabled Kaplan and Mahanti to explain the change in the slope of the separation boundary between the black and golden phases on the $PT$ diagram.[6] This explanation remains in force in our model.

The transition to the golden phase of SmS is known to be accompanied by a reduction in the magnetic susceptibility of SmS by about 60%, but the susceptibility remains temperature-independent for $T < 50$ K. The absence of a paramagnetic Curie contribution due to $f^5(^6H_{5/2})$ states from our model can be naturally explained by the fact that the ground state (4.16) is still a singlet in the new phase. As far as $\chi$ $(T \to 0)$ is concerned, its magnitude is determined by two factors. First, the Van Vleck susceptibility

$$\chi_{VV} = 8N\mu_B |\langle h | g \rangle|^2 (E_{J=1}^h - E_{T=0}^g)^{-1} \qquad (5.2)$$

of the golden phase can be reduced by the increase in the separation between the lowest level $E_{J=0}^g$ and the excited (exciton) term $E_{J=1}^h$ because the less localized orbitals (4.16) are more sensitive to the crystal field than the $f$-functions in the black phase. If the excited states $E^h$ lie in the continuum because of the reduction in the dielectric gap for $P > P_c$, the susceptibility $\chi_{vv}$ may also fall as a result of the reduction in the overlap integral between the radial parts of the wave functions in the ground and excited states $\langle h | g \rangle$. Second, our assumption that a heavy-hole band is present forces us to

take into account the Pauli contribution $\chi_P$ made by this band to the susceptibility. In general, the temperature dependence of this contribution is indistinguishable from the Van Vleck contribution for similar energy parameters. The result $\gamma = 145$ mJ/mole $\cdot$ deg corresponds to a susceptibility $\chi_P = 1.85 \cdot 10^{-3}$ cm³/mole (in the free-electron approximation). The experimental result is $\chi(T \to 0) \approx 3 \cdot 10^{-3}$ cm³ mole, which is in reasonable agreement with this corrected value if we recall that, in reality, both $C$ and $\chi$ are renormalized by the interaction. It may therefore be considered that the susceptibility of the golden phase is essentially of the Pauli type, and the width of the corresponding hole band is about 100 K, which is in good agreement with specific-heat data.

The weak point of this interpretation of low-temperature thermodynamic properties of the system is its dependence on the presence of acceptor levels in SmS. There is no doubt that such levels are present,[3,25,26] but it is meaningful to associate them with the thermodynamics of of the golden phase only if the acceptor levels are due to residual intrinsic defects whose concentration is always greater than the concentration of random donors. It is known that the kinetic properties of the black phase are very sensitive to stresses produced in the system,[25,29] and this enables us to suggest that structural defects with acceptor action are also produced during the phase transition, with a jump in the volume that is sufficient to have a decisive effect on the low-temperature properties of the golden phase of SmS.

We shall now explain how our model can exhibit the second phase transition that is observed at high pressures $P \sim 20$ kbar.[1–3] The reduction in residual resistance by an order of magnitude would appear to indicate that a transition has taken place to the normal metallic phase, but the overall form of the temperature dependence of resistance shows that the situation is not so simple.[2] The function $R(T)$ has the characteristic shape of the "spine of the Anderson elephant" with a maximum at $T \sim 10$–$20$ K, a quadratic temperature dependence as $T \to 0$, and a logarithmic dependence at high temperatures. In the language of the model of Fig. 5c, complete ejection of a single electron from the $f$-shell into the conduction band signifies a Mott-Hubbard transition in the band $\varepsilon_{ex}$ ($f^6 + f^5 d_t$), the result of which is that the number of places in the band increases by a factor of two.[9] However, the $f$-shells of the Sm atoms must then go over into the state $f^5(^6H_{5/2})$ with localized angular momenta. The fact that the ground state of the system remains nonmagnetic under these conditions signifies that the high pressure SmS phase is a "Kondo lattice" of the same kind as the CeAl$_3$.

The mechanism of the phase transition during the dissolution in SmS of divalent Y or Gd impurities (chemical collapse) is outwardly similar to the pressure-induced transition, but all evidence points to the fact that it is completely different. If we base ourselves on the temperature dependence $R(T)$, the compound $Sm_{1-x}Me_x^{3+}S$ is an ordinary "dirty" metal. More specifically, in the light of the ideas developed here and in Ref. 9, chemical collapse requires separate analysis, but we note that the substitution of $Y^{3+}(Gd^{3+})$ for $Sm^{2+}$ does not facilitate but, on the contrary, impedes the formation of excitons. The charged substituent

impurity breaks up the electron-hole pairs by its Coulomb potential, as was noted by Zittartz[30] as far back as 1967. Second, it disturbs the coherence of the narrow exciton band because, by releasing an electron into the conduction band, it does not produce a hole in the valence band, since each substituted atom signifies a loss of one level in the "Hubbard" band $\varepsilon_k^{(h)}$ in the Hamiltonian (3.1). For this reason, during chemical collapse, SmS undergoes a transition to the metallic phase and bypasses the mixed-valence state.

To summarize, our model provides a definite answer to the question of whether the golden phase of SmS is a metal or a dielectric. The answer is that this is a narrow-gap $p$-type semiconductor with an unusual, very narrow valence band that is responsible for practically all the puzzling properties of the system, such as the absence of Curie paramagnetism, metallic behavior of high-frequency permittivity but semiconductor-type static $\varepsilon_0$, negative slope of the phase separation line on the $PT$ diagram, complicated shape of the temperature dependence of resistivity, and, finally, the mixed valence itself. It is probable that the foregoing discussion can, essentially, be extended to $SmB_6$.

The author is indebted to B. A. Volkov, L. A. Maksimov, and D. I. Khomskiĭ for constructive criticism and valuable advice.

---

[1)]The appearance of the last term in (2.9) can be explained in terms of the nondegenerate model in which the $f^6$ and $f^5$ configurations are modeled by the $s^2$ and $s^1$ states. The mixing (2.4) then corresponds to processes of the form $f_{m\sigma} + f_m^+ - f_{m-\sigma}d_{n-\sigma}$, and the "supermixing" $\eta$ in (2.9) corresponds to processes of the form $f_{m\sigma} + f_{n-\sigma}^+ - f_{n-\sigma}d_{n-\sigma}$. Strictly speaking, supermixing need only include charge fluctuations $Z_n^{00} - \langle Z_n^{00} \rangle$, and the mean field can be included in the original hybridization (2.4). However, we shall neglect mean-field effects because they do not affect the overall picture of the phase transition.

---

[1]F. Holtzberg and J. Wittig, Solid State Commun. **40**, 315 (1981).

[2]F. Lapierre, M. Ribault, F. Holtzberg, and J. Floquet, Solid State Commun. **40**, 347 (1981).

[3]M. Konczukowski, J. Morillo, and H. P. Senateur, Solid State Commun. **40**, 517 (1981).

[4]R. M. Martin and J. W. Allen, J. Appl. Phys. **50**, 7561 (1979).

[5]T. A. Kaplan, S. D. Mahanti, and M. Barma, Valence Instabilities and Related Narrow-Band Phenomena, ed. By R. D. Parks, New York, 1977, p. 153.

[6]T. A. Kaplan and S. D. Mahanti, J. Appl. Phys. **49**, 2084 (1978).

[7]O. V. Farberovich, Fiz. Tverd. Tela (Leningrad) **21**, 3434 (1979) [Sov. Phys. Solid State **21**, 1982 (1979)].

[8]K. A. Kikoin and V. N. Flerov, Zh. Eksp. Teor. Fiz. **77**, 1062 (1979) [Sov. Phys. JETP **50**, 535 (1979)].

[9]K. A. Kikoin, Solid State Commun. **33**, 323 (1980).

[10]R. Ramirez, V. Falicov, and J. C. Kimball, Phys. Rev. B **2**, 3383 (1970).

[11]A. Z. Bringer, Z. Phys. B **21**, 21 (1975).

[12]J. Schweitzer, Phys. Rev. B **13**, 3506 (1976).

[13]M. Iwamatzu, Physica (Utrecht) B **106**, 415 (1981).

[14]Y. Kuroda and K. H. Bennemann, J. Phys. Soc. Jpn. **51**, 776 (1982).

[15]I. Egri, J. Phys. C. **12**, 1843 (1979).

[16]R. R. Gusseĭnov and L. V. Keldysh, Zh. Eksp. Teor. Fiz. **63**, 2255 (1972) [Sov. Phys. JETP **63**, 1193 (1972)].

[17]B. A. Volkov and V. V. Tugushev, Dokl. Akad. Nauk SSSR Ser. Fiz. **265**, 1374 (1982) [Sov. Phys. Doklady **27**, 836 (1982)].

[18]K. W. H. Stevens: a) J. Phys. C **9**, 1417 (1976); b) ibid. **11**, 985.

[19]B. H. Brandow, Solid State Commun. **39**, 1233 (1981).

[20]P. Fazekas, Z. Phys. B **47**, 301 (1982).

[21]C. Herring, in: Magnetism, ed. by T. Rado and H. Suhl, Vol. 2B, 1966, p. 1.

[22]P. W. Anderson and S. T. Chui, Phys. Rev. B **9**, 3229 (1974).

[23]A. N. Kocharyan and D. I. Khomskiĭ, Zh. Eksp. Teor. Fiz. **71**, 767 (1976) [Sov. Phys. JETP **44**, 404 (1976)].

[24]T. L. Bzhalava, M. L. Shubnikov, S. G. Shul'man, A. V. Golubkov, and I. A. Smirnov, Fiz. Tverd. Tela (Leningrad) **18**, 3148 (1976) [Sov. Phys. Solid State **18**, 1838 (1976)].

[25]A. V. Golubkov, E. V. Goncharev, V. A. Kapustin, M. V. Romanov, and I. A. Smirnov, Fiz. Tverd. Tela (Leningrad) **22**, 3561 (1980) [Sov. Phys. Solid State **22**, 2086 (1980)].

[26]J. Morillo, M. Konczukowski, and J. P. Senateur, Solid State Commun. **35**, 931 (1980).

[27]F. Holtzberg and J. Torrance, AIP Conf. Proc. **5**, 860 (1972).

[28]D. McWhan, S. M. Shapiro, J. Eckert, H. A. Mook, and R. J. Birgenau, Phys. Rev. B **18**, 3623 (1978).

[29]S. D. Bader, N. F. Phillips, and D. B. McWhan, Phys. Rev. **7**, 4686 (1973).

[30]J. Zittartz, Phys. Rev. **164**, 575 (1967).

Translated by S. Chomet